Available online at www.sciencedirect.com
SciVerse ScienceDirect
Scripta Materialia 68 (2013) 889–892
Scripta MATERIALIA
www.elsevier.com/locate/scriptamat

Microstructure and mechanical properties of ZrB_2–SiC–BN composites fabricated by reactive hot pressing and reactive spark plasma sintering

Wen-Wen Wu,[a,*] Wen-Long Xiao,[b] Mehdi Estili,[a] Guo-Jun Zhang[c] and Yoshio Sakka[a,*]

[a] *Advanced Ceramics Group, National Institute for Materials Science (NIMS), Tsukuba, Ibaraki 305-0047, Japan*
[b] *Surface Kinetics Group, National Institute for Materials Science (NIMS), Tsukuba, Ibaraki 305-0047, Japan*
[c] *State Key Laboratory of High Performance Ceramics and Superfine Microstructures, Shanghai Institute of Ceramics, Shanghai 200050, China*

Received 7 January 2013; revised 11 February 2013; accepted 11 February 2013
Available online 18 February 2013

ZrB_2–SiC–BN composites were fabricated from a powder mixture of ZrH_2, Si_3N_4 and B_4C via reactive hot pressing (RHP) and reactive spark plasma sintering (R-SPS). The phase composition, density, microstructure and mechanical properties of the final products were studied and compared. The sample fabricated by the R-SPS process showed higher density, flexural strength and fracture toughness and had a more homogeneous microstructure compared to the one fabricated by the RHP process.

Keywords: Borides; Reactive sintering; Spark plasma sintering

Because of their high melting point, excellent strength and oxidation resistance, ZrB_2–SiC-based composites are recognized to be the baseline of ultrahigh-temperature ceramics for applications in high thermal protection systems of hypersonic aerospace vehicles [1]. However, the fracture toughness and thermal shock resistance of these ceramics still need to be improved for practical applications. Improvements have been made by introducing layered materials with weak interlayer interactions and low Young's moduli, such as hexagonal boron nitride (h-BN) [2] and graphite [3,4], into the matrix. BN has been widely used to improve the thermal shock resistance of monolithic Si_3N_4 and SiC ceramics [5–7]. However, directly introducing BN leads to agglomeration or formation of large particles/platelets that could act as strength-limiting flaws and ultimately decrease the strength.

Reactive sintering has been found to be an effective way to fabricate composites with homogeneous dispersion of BN. Strain-tolerant SiC–BN composites were simultaneously synthesized and densified via the in situ reaction of Si_3N_4, B_4C and C during hot pressing (HP) [8]. On the other hand, reactive sintering has already been used to fabricate various ZrB_2–SiC-based composites with controlled microstructures from elemental powder mixtures or Zr–B_4C–Si powder mixtures [9–14]. Therefore, it is possible to fabricate ZrB_2–SiC–BN composites through the reaction of Zr, Si_3N_4 and B_4C following:

$$4Zr + Si_3N_4 + 3B_4C \rightarrow 4ZrB_2 + 3SiC + 4BN \quad (1)$$

Spark plasma sintering (SPS) is an advanced processing technique developed to consolidate ceramics and ceramic-based composites [15,16]. Unlike the HP process, SPS involves applying a pulsed electric current through the die and/or powder, leading to a rapid heating of the powder, which can result in improved densification and fine-grained products in shorter times and at lower temperatures. Bellosi et al. [17] reported that dense HfB_2–SiC and ZrB_2–ZrC–SiC ceramics could be obtained without the addition of sintering aids (HfN, Si_3N_4) and in a shorter time by using SPS, which cannot realized by the HP process. Moreover, the beneficial effect of the SPS technique was assessed by the improvement of the high-temperature strength.

Reactive SPS (R-SPS), a combination of reactive sintering and SPS, has been also attracting significant interest for the fabrication and rapid consolidation of

---

* Corresponding authors. E-mail addresses: wu.wenwen@nims.go.jp (W.-W. Wen); sakka.yoshio@nims.go.jp (Y. Sakka)

1359-6462/$ - see front matter © 2013 Acta Materialia Inc. Published by Elsevier Ltd. All rights reserved.
http://dx.doi.org/10.1016/j.scriptamat.2013.02.022

nanocomposites of various materials [18]. However, there have been few reports to date comparing the synthesis, microstructure and mechanical properties of the materials fabricated by RHP and R-SPS [11], and the influence of electric field on the reaction and sintering is not clear either. Here, we studied and compared the microstructure and mechanical properties of ZrB_2–SiC–BN composites fabricated by RHP and R-SPS processes according to the reaction (1).

Four ZrB_2–SiC–BN composites with various BN loadings were prepared. ZrH_2 (5 μm, purity 98%, Kojundo Chemical Laboratory Co., Ltd., Japan), Si_3N_4 (UBE SNE10, Japan) and B_4C (Grade HS, H.C. Starck, Berlin, Germany) were used to synthesize ZrB_2–SiC–BN composite with 30 vol.% BN phase. Powders were mixed in ethanol and ball-milled using Si_3N_4 balls for 24 h in a polyethylene bottle. The mixture was then dried in air. For the RHP process, the mixed powders were placed in a graphite die, then heated at a slow heating rate (10 °C min^{-1}) to 2000 °C and held for 60 min under a pressure of 20 MPa in vacuum. The R-SPS process was carried out with a, SPS furnace (100 kN SPS-1050, Syntex Inc., Japan) in a vacuum with a heating rate of 50 °C min^{-1}, and a load of 40 MPa was applied. The sintering temperature was 1900 °C and the holding time was 5 min.

The predicted composition is 46 vol.% ZrB_2–24 vol.% SiC–30 vol.% BN, with a theoretical density of 4.20 g cm^{-3} based on the rule of mixture. The densities of the as-prepared samples were measured by the Archimedes method. The phase compositions were identified by an X-ray diffraction (XRD) analyzer (Model RINT 2500, Rigaku Co., Tokyo, Japan, 40 kV ~ 300 mA) with Cu K_α radiation. The microstructures of the samples were investigated by scanning electron microscopy (SEM) (JSM-6500F, JEOL Ltd., Japan) and transmission electron microscopy (TEM) (JEM-2100, JEOL Ltd.). A three-point flexural strength test at room temperature was conducted on a mechanical strength testing system (Model 4505, Instron Corp., MA), using 2 mm × 1.5 mm × 18 mm chamfered bars with a 16 mm span and a crosshead speed of 0.5 mm min^{-1}. The fracture toughness was evaluated by a single-edge notched beam test with a 16 mm span and a crosshead speed of 0.05 mm min^{-1} using 2 mm × 4 mm × 18 mm test bars; the notch was about 2 mm deep and 0.14 mm wide. The hardness was determined by Vickers indentation (MVK-E, Akashi Co., Japan) under a load of 98 N for 15 s. All the reported strength, toughness and hardness values are the average of five reliable measurements.

Figure 1(a) shows clear ZrB_2, β-SiC and h-BN peaks of composite fabricated by R-SPS at 1900 °C for 5 min; no other phase was observed. In contrast, the h-BN peaks in the composite prepared by the RHP process at 2000 °C for 60 min (Fig. 1(b)) are significantly weaker, with the strongest peaks intensity ratios ($I_{BN,(002)}/I_{ZrB_2,(101)}$) of 1.4 and 7.2 for the RHPed and R-SPSed ZrB_2–SiC–BN composites, respectively. Meanwhile, peaks of ZrC phase can also be observed in the latter case. Although the RHP process was conducted under a higher sintering temperature and with a longer holding time than R-SPS, the RHPed sample was not as dense as the R-SPSed sample (see Table 1). The flexural strength and fracture toughness of the R-SPSed sample are 457.7 ± 26.4 MPa and 4.3 ± 0.1 MPa $m^{1/2}$, respectively, which are 100.3 and 72.0% higher than those of RHPed samples (228.4 ± 22.1 MPa and 2.5 ± 0.2 MPa $m^{1/2}$). Due to the existence of 30 vol.% h-BN, the hardness values of the R-SPSed and RHPed samples (3.1 ± 0.1 GPa and 3.5 ± 0.5 GPa, respectively) are highly comparable, though considerably lower than those of traditional ZrB_2-based ceramics (21–23 GPa [19]).

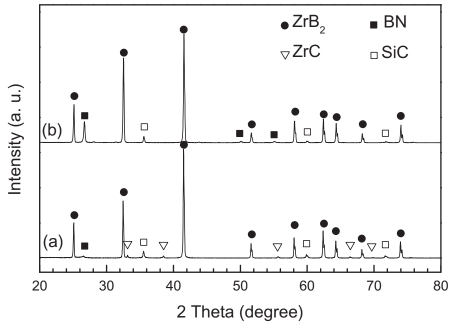

Figure 1. XRD patterns of the ZrH_2–Si_3N_4–B_4C mixture: (a) R-SPSed at 1900 °C for 5 min; (b) RHPed at 2000 °C for 60 min.

In order to understand the differences in phase composition, density and mechanical properties of the samples synthesized by the different reactive sintering methods, the microstructure of the samples was studied by SEM and TEM. The microstructure of the R-SPSed ZrB_2–SiC–BN composites is more homogeneous than the RHPed sample, as shown in Figures 2 and 3(a–c). No obvious agglomeration can be observed in the R-SPSed material, in which large h-BN grains (1–3 μm) with a layered structure are uniformly located at the boundaries of ZrB_2 and SiC grains. As for the RHPed material, the size of the h-BN grains are much smaller (<1 μm), but large ZrB2-rich and h-BN-rich agglomerates can be easily observed throughout the sample. The ZrB_2 and SiC grains in both materials showed an equiaxed morphology. The grains in the ZrB_2-rich area of the RHPed sample (Fig. 3 (b)) have an average size of ~2 μm for ZrB_2 and ~1 μm for SiC, which are very similar to those of the R-SPSed composite (Figs. 2(a) and 3(a)).

In addition to ZrB_2, SiC and h-BN, the existence of oxide impurities was also detected in both composites, as shown in Figure 3(a), (c) and (d). The diffraction patterns of the circled areas in Figure 3(a) and (c) indicate that the impurities are mainly monolithic ZrO_2 (space group *P21/c*). The energy-dispersive X-ray spectra of the ZrO_2 grain in Figure 3(d) are shown in Figure 3(e). Characteristic peaks of Zr, O, B and C were present inside the ZrO_2 phase. In addition, an amorphous intergranular film is present at the grain boundary of ZrB_2 and ZrO_2, as shown in Figure 3(f). The concentration of the oxide impurities is much lower in the R-SPSed composite than in the RHPed one. The ZrO_2 phase in the former contains mainly spherical particles with diameters <1 μm (Fig. 3(a)), while the ZrO_2 scale in the microstructure of the latter has an irregular shape and a significant larger size of several microns (Fig. 3(c)).